

to happen would be if a reasonable fraction ($\sim 36\%$) of the sample were actually Eu_2S_3 . However, an x-ray study of the EuS powder revealed no detectable trace of a second phase. Since the transmission effects in Eu metal and EuS are of the same sign, so are the effective fields. The field in the metal is thus also negative, as has generally been assumed. Any conduction electron effects are thus contained in the difference between $H_{\text{hfs}} = -329$ kOe in EuS and $H_{\text{hfs}} = -264$ kOe in the metal (both values are corrected to 0°K).

We had originally hoped to be able to see the direct effect of H_{app} on \mathcal{E} . Since H_{hfs} is negative, lowering H_{app} from 15 to 9 kOe would in principle have caused an increase of 2.5% in \mathcal{E} . This would be just detectable, were it not for the fact that there are uncertainties introduced

by the field dependence of the depolarization correction and the spin-lattice relaxation.

ACKNOWLEDGMENTS

The authors are indebted to T. R. McGuire of the IBM Watson Research Center for suggesting the use of EuS in this experiment and to M. W. Shafer of that laboratory for preparing the material. J. J. Hurst of BNL, who was continually helpful during the sample fabrication, provided the x-ray analysis. The technical assistance of R. D. Schmidt, W. K. Kristiansen and R. Smith is greatly appreciated. Finally, P. Kienle of the Technischen Hochschule München was our guest during the planning stages of this work and contributed greatly to the early discussions.

Trapping Centers in Thermoluminescent Calcite

W. L. MEDLIN

Socony Mobil Oil Company, Inc., Field Research Laboratory, Dallas, Texas

(Received 30 April 1964; revised manuscript received 23 May 1964)

Trapping levels which account for most of the thermoluminescence in natural calcite have been investigated. Results are based on a study of color centers which are shown to be closely associated with the traps involved in thermoluminescence. Optical absorption measurements in a variety of Iceland-spar crystals show that the prominent calcite glow peaks at 350, 500, 600, and $\sim 700^\circ\text{K}$ are accompanied by thermal bleaching of the color centers. Results indicate that the color centers are due to one kind of trapped-hole center and at least four kinds of trapped-electron centers. Recombinations resulting from thermal bleaching of each of these centers excites emission at Mn^{++} impurity ions and produces the observed glow peaks. The mechanism for exciting the Mn^{++} ions appears to be the same nonradiative transfer process which accounts for sensitized luminescence in calcite.

I. INTRODUCTION

Thermoluminescence in natural calcite is usually associated with the presence of divalent manganese, a common impurity.¹ There are three prominent glow peaks in most samples at 350, 500, and 600°K and a weaker peak near 700°K . The orange emission of these glow peaks is produced by the ${}^4G(T_{1g}) \rightarrow {}^6S$ transition in the Mn^{++} ion,² which occupies substitutional sites in the lattice.³ This transition is forbidden so it cannot be directly excited by optical absorption. But indirect excitation through host lattice absorption of ionizing radiation is possible; and it is by this method that luminescence is produced. Another form of indirect excitation occurs through the action of sensitizing agents such as Pb, Tl, or Ce. These impurities absorb radiation in their own characteristic absorption bands and transfer energy through a nonradiative, resonance mechanism to Mn^{++} centers. This produces

sensitized luminescence,⁴ which has the same emission characteristics as thermoluminescence and x-ray excited luminescence.

Trapping centers in calcite are somewhat analogous to sensitizing ions. Both provide indirect processes for exciting the forbidden Mn^{++} transitions. The properties of sensitizing centers in calcite have been studied in detail.⁴ But comparatively little is known about the trapping centers or about the mechanism for exciting emission when the traps are emptied.

There is good evidence that the traps which produce thermoluminescence are associated with color centers. Thermoluminescent crystals are visibly darkened by x-ray irradiation whereas nonthermoluminescent crystals remain uncolored. This suggests that a study of the relation between color centers and thermoluminescence may provide information about trapping centers associated with the glow peaks.

In this paper we describe the results of an investi-

¹ W. L. Medlin, *J. Chem. Phys.* **30**, 451 (1959).

² W. L. Medlin, *J. Opt. Soc. Am.* **53**, 1276 (1963).

³ F. K. Hurd, M. Sachs, and W. D. Hersberger, *Phys. Rev.* **93**, 373 (1954).

⁴ J. H. Schulman, L. W. Evans, R. J. Ginther, and K. J. Murata, *J. Appl. Phys.* **18**, 732 (1947); C. C. Klick and J. H. Schulman, *Solid State Physics*, edited by F. Seitz and D. Turnbull (Academic Press Inc., New York, 1957), Vol. 5, p. 123.

gation directed along these lines. In addition to absorption and emission properties, we have also investigated changes in electrical conductivity of thermoluminescent crystals during heating.

II. EXPERIMENTAL PROCEDURE

The connection between color centers and thermoluminescence was investigated by studying absorption changes during heating. Thermal bleaching curves were measured simultaneously with glow curves over the range, 90–850°K. The results, which showed bleaching stages accompanying each prominent glow peak, were analyzed in terms of polarized absorption spectra, measured after each bleaching stage. The kinetics of bleaching and emission were studied by measuring isothermal decay of absorption together with decay or phosphorescence.

To determine whether the emptying of traps is an ionization process, changes in electrical conductivity were measured concurrently with the glow curve. Similar measurements have already been reported by Rao⁵ in thermoluminescent single crystals of calcite. He observed an increase in conductivity during the 350°K glow peak and concluded that ionization occurred. However, his conductivity data were based on changes in high-frequency dielectric loss. Others have shown⁶ that such measurements are not conclusive evidence of a charge-transfer process; at high frequencies, losses due to the traps themselves, produce changes in loss factor for any trap-emptying mechanism. Therefore, Rao's data could be explained as well by a localized process as by an ionization mechanism.

For the present investigation, dc measurements were made on single crystals heated from room temperature. In calcite, as in most other ionic crystals, dc polarization effects are troublesome for ionic currents above $\sim 10^{-12}$ $\Omega^{-1} \text{ cm}^{-1}$. To eliminate this problem, pulse techniques were used. This reduced the sensitivity of the measurements somewhat, but it was still possible to detect ionic currents just above room temperature. Therefore, the conclusiveness of the results was still limited by interference from ionic conductivity rather than sensitivity of the measurements.

III. APPARATUS

All single crystal absorption spectra were measured at low temperature with a Beckman DK-2A recording spectrophotometer. A conventional stainless-steel, liquid-nitrogen Dewar with quartz windows was used for cooling the sample. A beryllium window was provided for irradiating the crystal at low temperature. A thermocouple, cemented into a representative crystal, showed that the average sample temperature was $90 \pm 3^\circ \text{K}$ when the Dewar was filled with liquid nitrogen.

Measurements involving quantitative determination of absorption coefficient were made with crystals 2 mm thick. For other measurements crystals of 2–5-mm thickness were used. All samples were irradiated by x rays from a Mo tube operated at 35 kV and 20 mA.

Thermal bleaching curves were measured in two stages: from 90–600°K, and from room temperature to 800°K. The Dewar system was used for the low-temperature range; a pair of cartridge heaters mounted just above the sample block warmed the crystal at a rate of 0.5 deg/sec and a thermocouple soldered into the sample block was calibrated to read temperature of the crystal. For the high-temperature range, the Dewar was replaced by a brass heater block on which the crystal was mounted in air. Temperature was again measured by a thermocouple located near the crystal and the same heating rate was used. A 5819 photomultiplier positioned above the crystal measured thermoluminescence. A Corning 7-54 filter was placed in front of the spectrophotometer detector during all measurements to eliminate effects of thermoluminescence and incandescent glow during heating.

To measure simultaneous decay of absorption and phosphorescence at room temperature the crystals were mounted in air on an aluminum block. The temperature in the sample compartment was controlled by cooling water which was regulated to $\pm 0.5^\circ$. This provided temperature regulation in the sample compartment to $\pm 0.2^\circ$. A 5819 photomultiplier mounted above the crystal measured phosphorescent decay. With this system the decay of absorption could be followed in most crystals for 30–40 h. However, phosphorescent decay could not be measured for more than about 2 h because of sensitivity limitations. Longer phosphorescent decay curves were obtained separately by cementing the crystals directly onto the face of a 1P28 photomultiplier. These measurements were made in a constant temperature room where fluctuations were less than 0.5° .

During measurements made with the recording spectrophotometer, the crystal was necessarily exposed to light throughout the decay period. For decay measurements in the dark a Beckman DU manual spectrophotometer was used with the crystal positioned out of the light beam between readings.

For most of the absorption measurements it was desirable to use light polarized parallel, or perpendicular to, the *c* axis of the crystal. For this purpose the spectrophotometer was equipped with a Glan-Thomson air gap prism whose transmission extended to 2200 Å. The prism was mounted so that its direction of polarization could be rotated through 360° in a plane perpendicular to the light path. The crystals were properly oriented by grinding faces parallel to the (0001) and (01 $\bar{1}$ 0) planes. They were then mounted with the (0001) face parallel and the (01 $\bar{1}$ 0) face perpendicular to the light path. Orientation of the crystal faces was checked

⁵ K. V. Rao, *Phys. Chem. Solids* **20**, 193 (1961).

⁶ G. F. J. Garlick and A. F. Gibson, *Proc. Roy. Soc. (London)* **A188**, 485 (1947).

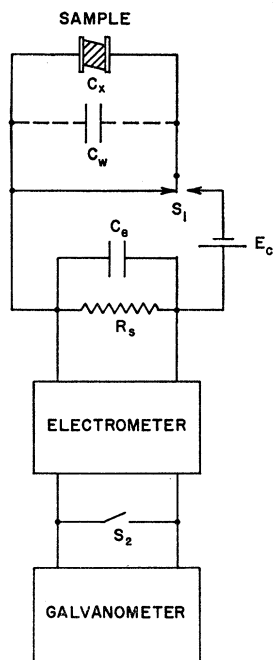


FIG. 1. Circuit for pulsed dc conductivity measurements.

with a petrographic microscope equipped with Bertrand lens and universal stage.

The circuit for pulsed dc conductivity measurements is shown in Fig. 1. The crystal sample, clamped between a pair of spring loaded, silver electrodes, was normally short circuited through S_1 . At regular intervals a thyatron control circuit switched S_1 to its alternate position. This removed the short circuit and applied a voltage E_c across the crystal. A Keithley Model 200B electrometer, with shunt resistance R_s , detected the resulting current flow. The electrometer output was wired to a sensitive galvanometer which was shunted by a second switch S_2 . The purpose of S_2 was to allow the wiring and sample capacitances C_w and C_x to be charged before the electrometer signal was applied. The electrometer capacitance C_e remained charged at all times. After a suitable delay the thyatron switching mechanism opened S_2 for an appropriate time, then closed it and returned S_1 to the shorted position.

The total pulse length was the charging time for C_w and C_x , added to the time required for the electrometer signal to produce a suitable galvanometer deflection. C_w and C_x , which were a few $\mu\mu\text{F}$ each, were charged through R_s , which determined the electrometer sensitivity. By limiting R_s to $10^7 \Omega$ it was possible to use a 0.1-sec pulse and still retain a sensitivity of 3×10^{-12} A per mm of galvanometer deflection.

The measurements were made at 30-sec intervals as the crystal and holder were heated at a linear rate of 0.5 deg/sec in a tubular furnace. The heating cycle was started at room temperature and the pulse polarity was reversed after each measurement. The crystals were cleaved and ground to dimensions of 3 mm on each edge and all measurements were made between cleavage

faces. The most reproducible results were obtained by evaporating silver or aluminum films on the faces in contact with the electrodes. Thermoluminescence was measured by a 5819 photomultiplier located a few inches from the crystal.

IV. RESULTS

A. Absorption Measurements

Most of the absorption induced in calcite by ionizing radiation is due to a pair of broad, uv absorption bands centered near 2900 and 3500 Å.^{5,7,8} On the basis of polarized absorption measurements, the 2900-Å band has been attributed to CO_3^- centers and the 3500-Å band to Ca^+ centers. Both bands are bleached at a measurable rate at room temperature. The decrease in absorbance has been correlated with decay of an orange phosphorescence⁸ which can be attributed to Mn^{++} emission associated with the 350°K glow peak.^{2,9}

Absorption spectra of a large number of natural crystals showed that there were generally three types. Nonthermoluminescent crystals were only slightly colored and the spectra consisted of a variety of low-intensity uv bands. Thermoluminescent crystals of good quality gave spectra quite similar to those reported in the literature. Poor quality thermoluminescent crystals gave somewhat different and more variable spectra. Both types of thermoluminescent crystals showed evidence of other uv absorption bands besides those near 2900 and 3500 Å. These were better resolved after heating the crystals to temperatures high enough to produce partial thermal bleaching.

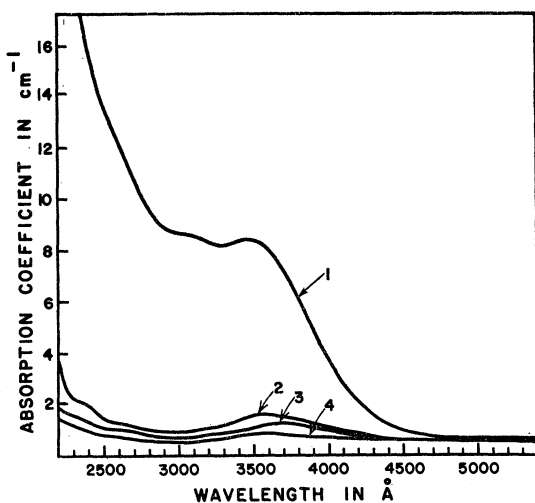
Polarized absorption spectra for two representative crystals, irradiated at 90°K, are shown in Figs. 2 and 3. The curves of Fig. 2 were typical of good quality crystals with few flaws and relatively low Mn^{++} content (<100 ppm). Crystals of poorer quality with higher Mn^{++} content (>1000 ppm) gave absorption spectra like those in Fig. 3; although the results were somewhat variable in different crystals.

The good quality crystals are colored rather slowly under x-ray irradiation and have only moderately intense glow peaks. There are strong absorption bands near 2950 and 3500 Å, and weaker bands near 3100, 2600, and 2300 Å. The weak bands are better resolved after the crystals have been heated to temperatures high enough to produce partial thermal bleaching. Orienting the E vector perpendicular, or parallel to the c axis shows the previously reported dichroism⁸ in the 2950-Å band. The 3500-Å band has little or no dichroism, and the same appears to be true of the 3100-, 2600-, and 2300-Å bands. However, the last two are shifted slightly as the E vector is rotated.

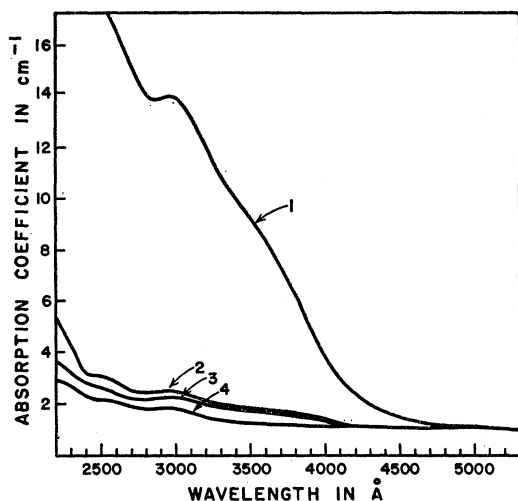
⁷ K. K. Sarsembaeva, Vestn. Akad. Nauk Kaz. SSR 18, 83 (1962).

⁸ W. F. Kolbe and A. Smakula, Phys. Rev. 124, 1754 (1961).

⁹ W. L. Medlin, Phys. Rev. 122, 837 (1961).



(a)



(b)

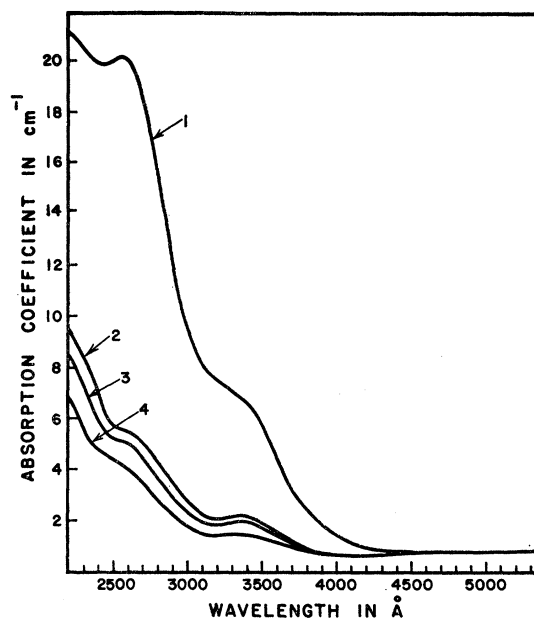
FIG. 2. Absorption spectra of a representative, good quality crystal with (a) E vector parallel to c axis, (b) E vector perpendicular to c axis: 1—after 7-h irradiation at 90°K , 2—after heating to 450°K , 3—after heating to 550°K , 4—after heating to 650°K .

The poor quality crystals are rapidly colored and have high-intensity glow peaks. In their absorption spectra, of which Fig. 3 is a typical example, the 3500-Å band is shifted to lower wavelength, usually between 3300 and 3400 Å. The 2950-Å band apparently moves to higher wavelength and is roughly superimposed on the 3100-Å band. The 2600- and 2300-Å bands are relatively more prominent, and are largely obscured, for $E \perp c$, by the strongly dichroic absorption edge.

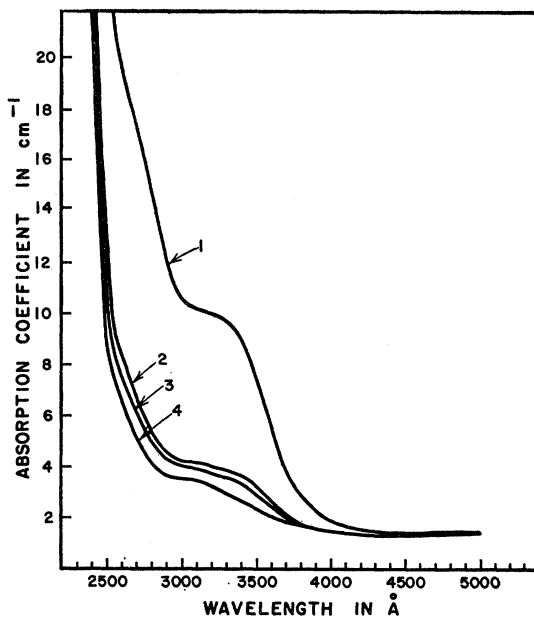
In all crystals the color centers appear to be completely stable at liquid-nitrogen or dry-ice temperature. Measurements in a representative crystal showed no loss in absorption at either of these temperatures over a 24-h period. The color centers were also stable at these temperatures under exposure to uv light. At room

temperature all absorption bands decayed at roughly equal rates, which were similarly unaffected by uv exposure.

The bleaching temperatures in Figs. 2 and 3 are appropriate for selectively emptying the traps associated with each of the prominent glow peaks at 350, 500,



(a)



(b)

FIG. 3. Absorption spectra of a representative, poor quality crystal with (a) E vector parallel to c axis, (b) E vector perpendicular to c axis: 1—after one-hour irradiation at 90°K , 2—after heating to 450°K , 3—after heating to 550°K , 4—after heating to 650°K .

600, and $\sim 700^\circ\text{K}$. The fact that each heating produces additional bleaching of all bands suggested that bleaching and glow occurred simultaneously. To investigate this in more detail we measured absorption at fixed wavelength simultaneously with thermoluminescence during heating. Results showed that each glow peak is accompanied by partial thermal bleaching of all absorption bands. Curves measured at 3500 \AA are shown in Figs. 4 and 5 for good and poor quality crystals, respectively. Similar curves were obtained at wavelengths corresponding to the other absorption maxima. These results show that thermoluminescence is clearly associated with annihilation of color centers.

There are significant differences in the glow curves of Figs. 4 and 5 which were characteristic of the good and poor quality crystals. Relative prominence and broadening of the 350°K glow peak are two such features. Also, the relative intensities of the 500 and 600°K glow peaks were consistently reversed for the two types of crystals. Moreover, in Fig. 4, the temperature of the last glow peak near 730°K varied by as much as 30° in different crystals; whereas, the corresponding peak in Fig. 5 always occurred at 680°K without variation. Glow curves like the one in Fig. 5 are characteristic of most calcite rock samples.

In crystals of both types there was evidence of a bleaching stage beginning near 800°K . However, the increased glow in this region of Figs. 4 and 5 is due to incandescent radiation from the sample block. Absorption measurements before and after heating several crystals to 870°K in a furnace also showed evidence of a small bleaching stage above 800°K . Crystals heated to 870°K still gave weak absorption in the $2600\text{--}3500\text{-\AA}$ region, even after heating to 1000°K in a CO_2 atmosphere.

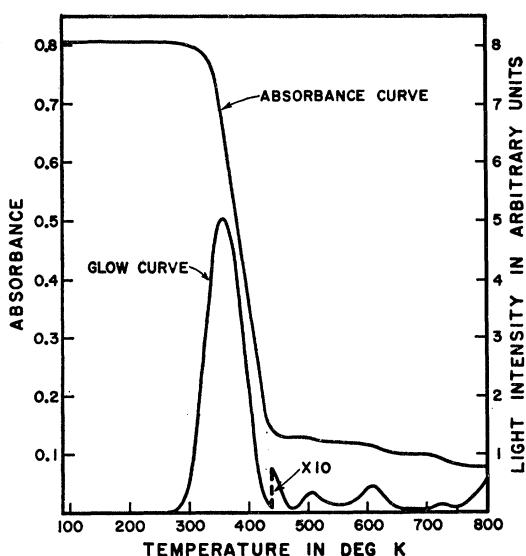


Fig. 4. Bleaching curve and simultaneously measured glow curve of a typical, good quality crystal irradiated for 7 h at 90°K .

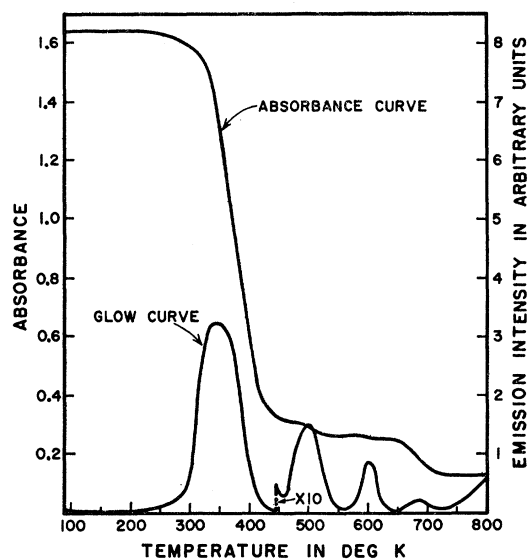


Fig. 5. Bleaching curve and simultaneously measured glow curve of a typical, poor quality crystal irradiated for 1 h at 90°K .

Figure 2(a) shows that in the good quality crystals each bleaching stage is accompanied by a shift in the 3500-\AA band. The first stage produces a shift from 3450 to 3550 \AA and succeeding stages move the band maximum to 3600 and about 3500 \AA , respectively. There was no measurable shift in any of the other bands.

Similar shifts are observed for the 3300-\AA band in Fig. 3. The wavelength changes were more difficult to estimate in this case because of interference from the 3100-\AA band. But the direction of change was obvious in all cases and agreed with the results in Fig. 2(a).

The relation between Mn^{++} emission and bleaching of absorption bands raises the question of whether the color centers are associated with Mn^{++} ions. We have investigated this possibility by comparing absorption data with colorimetrically determined Mn^{++} concentration in a number of crystals. Results showed no apparent correlation between x-ray induced absorbance and Mn^{++} content. On the other hand, we have found no crystals free of manganese which can be colored by x rays.

The curves of both Fig. 4 and Fig. 5 show an obvious decrease in number of Mn^{++} transitions produced per unit change of absorbance beyond the 600°K glow peak. This effect could be accounted for by assuming that radiationless transitions begin to predominate in the Mn^{++} centers above 600°K . However, Fig. 6, which is a plot of x-ray excited luminescence efficiency versus $1/T$, indicates that this effect alone is not sufficient to explain the results in Figs. 4 and 5. Apparently, a loss in efficiency of the mechanism for exciting Mn^{++} centers must also be assumed.

B. Decay Measurements

At room temperature all of the absorption bands decay simultaneously within a few days to the absorbance level corresponding to the end of the first bleaching stage in Figs. 4 and 5. The density of color centers associated with the other bleaching stages is not measurably decreased during this time. Optical bleaching is also insignificant; decay measurements made in the dark were identical, within the limits of error, to those made during exposure to light. Therefore, room-temperature measurements are particularly convenient for studying isothermal decay of absorbance associated with the first stage of thermal bleaching. Simultaneous measurement of phosphorescent decay provides additional information about the relation between bleaching and emission.

Decay of absorption and phosphorescence at room temperature have already been studied to some extent by Kolbe and Smakula.⁸ They attributed the phosphorescence to hole-electron recombinations produced by annihilation of the color centers. But it has been shown elsewhere^{2,9} that the emission is actually due to Mn⁺⁺ transitions associated with the 350°K glow peak.

The simplest relation to be expected between the two decay processes is a constant proportionality between rate of color center annihilation and rate at which Mn⁺⁺ transitions occur. The latter is proportional to emission intensity $I(t)$. And if it is assumed that changes in color center density are proportional to changes in absorption coefficient $\Delta\mu$, this would give

$$\Delta\mu = K \int_{t_1}^{t_2} I(t) dt. \quad (1)$$

Our measurements of $\Delta\mu$ and $I(t)$, obtained simultaneously at room temperature, follow this relation quite well for all crystals investigated. Figure 7 shows results for the 3500-Å band of a representative crystal during the first 90 min of decay, which was about the

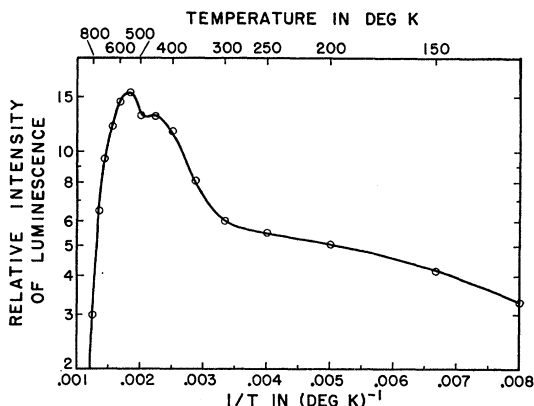


FIG. 6. X-ray excited luminescent efficiency versus $1/T$ for Mn-activated calcite.

maximum time that phosphorescence could be followed. The absorption measurements were made with unpolarized light at 3500 Å, starting at $t_1 = 1.0$ min.

The data in Fig. 7 can be used to calculate the oscillator strength of the 3500-Å band. According to the Gaussian form of Smakula's formula, the constant K , in Eq. (1), is related to oscillator strength f as follows:

$$K = \frac{cf(n^2+2)^2}{0.87 \times 10^{17} n W}, \quad (2)$$

where W is the half-width of the absorption band, n is the index of refraction, and c relates emission intensity to number of Mn⁺⁺ transitions per second. The value of c was determined by comparing the phosphorescence

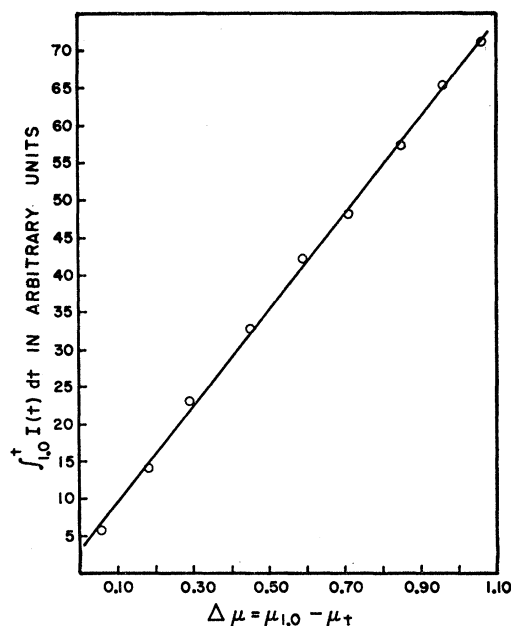


FIG. 7. Integrated intensity of phosphorescence versus change in absorption coefficient at 3500 Å during room-temperature decay of a representative crystal.

intensity with a standard source of known brightness. With Eq. (2) the f value can be determined from the slope of the $\Delta\mu$ versus $\int I dt$ plot. The data in Fig. 7, and results for a number of other crystals, give $f = 0.9 \pm 0.1$ for the 3500-Å band. The rather poor precision of this determination is due largely to the uncertainty in W . This quantity was determined by fitting a Gaussian curve to the 3500-Å absorption peak in Fig. 2(a).

The above f value has been used in Smakula's formula to calculate the approximate number of color centers annihilated during the first two bleaching stages of Figs. 4 and 5. Results for a number of crystals are given in the Δz column of Table I. These are compared with the corresponding number of radiative Mn⁺⁺ transitions Δx , associated with the 350 and 500°K glow peaks. The Δx values were computed from glow peak

areas using the conversion factor c . Also given are concentration of Mn^{++} ions N and x-ray excited luminescent intensity L . The latter can be taken as a measure of the relative fraction of Mn^{++} ions which contribute to glow peak emission.

The results in Table I show that surprisingly large fractions of color centers produce emission during bleaching. In one case $\Delta x > \Delta z$, although the difference is within limits of error. The results also show large variations in the relative fractions of centers bleached during each stage. In addition, the fraction which produces emission varies considerably in different crystals. Neither of these features can be correlated with N or L .

Decay of calcite absorption bands can be compared with the decline of F - and V -band absorption in alkali halides. In KCl, Damm and Tomkins have shown that the decay of F and V_2 bands follows the relation,¹⁰

$$\frac{k}{t} = \frac{1}{a_0 - a} - \frac{1}{a_0 - a_\infty} \quad (3)$$

The constants a_0 and a_∞ are the initial and final absorbance, respectively, and k is a rate constant; a is the total absorbance, or area under the absorption band, measured at time t after irradiation is ended. Equation

TABLE I. Approximate number of color centers annihilated Δz compared with number of manganese transitions Δx , number of manganese ions present N , and relative luminescent efficiency L . * means crystal was broken by heating.

Sample	N	L	Δz_{350}	Δx_{350}	Δz_{600}	Δx_{600}
14	2.8×10^{19}	0.49	2.0×10^{16}	1.1×10^{16}	0.42×10^{16}	0.17×10^{16}
18	3.6	0.45	1.8	0.52	0.33	0.028
30	3.1	0.30	2.3	0.37	*	*
32	4.1	0.49	2.1	0.94	0.21	0.0034
33	2.1	0.31	2.2	0.62	*	*
34	3.3	0.53	1.4	0.91	0.94	0.18
40	6.5	0.93	1.2	1.2	0.90	0.38
41	4.9	1.0	1.3	1.6	1.5	1.1
52	3.0	0.33	2.1	0.58	0.36	0.13

(3) can be accounted for by assuming a simple bimolecular recombination of F and V_2 centers with competitive trapping of F -center electrons by anion vacancies. The observed decay is obtained if the trapping probabilities of the V_2 centers and anion vacancies are approximately equal.

The room-temperature decay of all calcite absorption bands can be fitted to Eq. (3) reasonably well after the first 30–60 min. Figure 8 shows some representative results. The area under the absorption bands could not be measured with accuracy in this case so the peak absorbance was used instead.

The points plotted at $1/t=0$ in Fig. 8 were obtained by heating the crystals to 400°K. This is sufficient, according to Figs. 4 and 5, to bleach all color centers

¹⁰ J. Z. Damm and F. C. Tomkins, Discussions Faraday Soc. 31, 184 (1961).

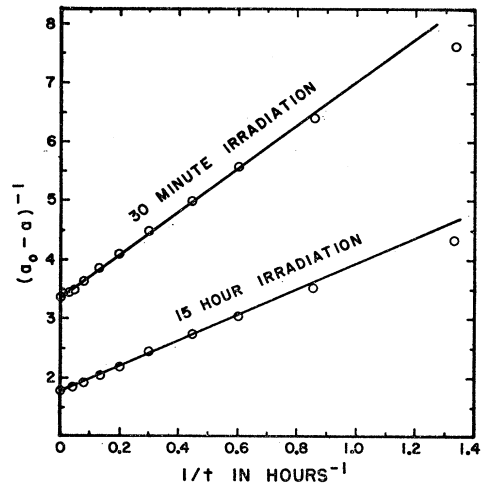


FIG. 8. Room temperature decay of absorbance at 3500 Å versus inverse decay time for a representative crystal.

associated with room-temperature decay, without affecting the others. These points coincide, as they should, with the intercepts $(a_0 - a_\infty)^{-1}$ of lines drawn through the other data points. However, the slope k of these lines changes with irradiation time, which is contrary to Eq. (3). This discrepancy, and the poor fit during the first 30–60 min of decay, show that bimolecular recombination is not totally consistent with the absorbance decay curves.

Even greater discrepancies are found in phosphorescent decay measurements. The decay of phosphorescence corresponding to Eq. (3) is

$$I = I_0 [kn_0 / (kn_0 + t)]^2, \quad (4)$$

where n_0 and I_0 are the number of color centers and the emission intensity when irradiation ceases. Decay curves covering periods of the order of 50 h gave results which could not be fitted to Eq. (4), but had the more general form,

$$I = I_0 [b / (b + t)]^\mu, \quad (5)$$

after the first 30–60 min of decay. In general, $\mu < 2$ and the change in b for different irradiation times is much smaller than the change in n_0 (as computed from absorption measurements). Figure 9 shows some decay curves for a representative crystal which illustrate this. The results are plotted as $\log I$ versus $\log(b + t)$ using values of b which give the best fit to straight lines for all but the first 30–60 min of decay. These data are further evidence that the bimolecular representation is only approximate.

C. Recombination Emission

It is clear from results given so far that thermoluminescence in calcite is an indirect emission produced at Mn^{++} sites by thermal bleaching of color centers. It is of interest to know whether a direct recombination

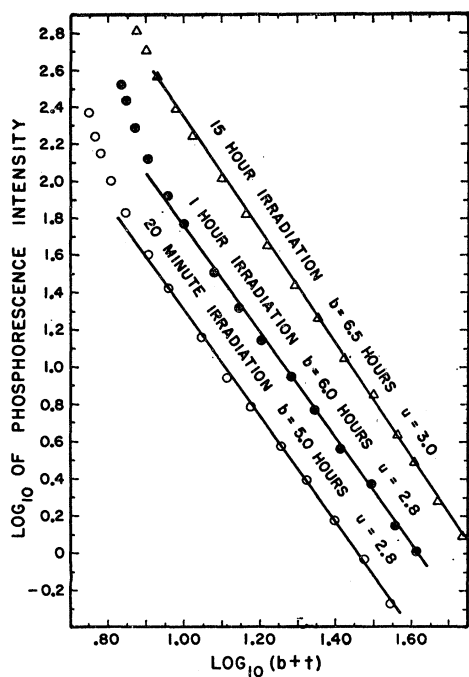


Fig. 9. Room-temperature decay of phosphorescence in a representative crystal.

emission is also produced by annihilation of the color centers. Obviously, this could best be observed in samples with lowest Mn^{++} content. For this purpose several synthetic samples were precipitated with Mn^{++} contents of no more than 2 ppm.

Figure 10 shows the glow curve produced by a one-hour irradiation of a representative sample of this group. Similar glow curves are produced by most natural crystals with very low Mn^{++} content. The features of interest are the prominent glow peak at 330°K and weaker peaks at 360 and 510°K. Measurements with a series of interference filters showed that the 360 and 510°K peaks are the usual ones due to Mn^{++} . The 330°K peak, on the other hand, has a broad emission spectrum which peaks somewhat below 3500 Å. A 3500-Å filter was used to study this glow peak in synthetic samples with higher Mn^{++} concentrations. Results showed rapid quenching with increasing Mn^{++} content; the peak was no longer detectable in samples with as little as 100 ppm manganese. On the basis of these results we attribute this glow peak to direct emission produced by recombinations during bleaching of the color centers.

D. Electrical Measurements

Conductivity curves for a number of crystals are shown in Fig. 11 as a function of temperature. Each sample was irradiated at room temperature for two hours and heated at a constant rate of 0.5 deg/sec. The curves are identified by the Mn^{++} content of each

crystal, which roughly determines the intensity of thermoluminescence in calcite.¹ With the exception of the 2 ppm sample, these crystals gave the deepest coloring and highest thermoluminescence intensity of the more than 40 specimens studied. All of them were the poor quality type whose absorption spectrum is represented by Fig. 3. The two-hour, room-temperature irradiation produced color center densities ranging from 10^{16} to 10^{17} cm^{-3} . There is no evidence, in any of the curves, of increased conductivity during the 350°K bleaching stage; and curves measured before irradiation were not significantly different from those in Fig. 11.

This indicates that the 350°K bleaching stage does not involve freeing of trapped charge carriers. However, this result is not conclusive without some evidence that currents produced in this way would be detectable above the ionic conductivity.

There are two possible bleaching mechanisms involving ionization of the color centers: (1) charge carriers freed from one kind of color center can recombine with the oppositely charged carriers at other color centers; or (2) both kinds of color centers can be ionized with the charge carriers subsequently recombining at Mn^{++} ions. For case (1) Mn^{++} emission would be produced by an indirect process such as energy transfer. For case (2), the Mn^{++} center would first capture charge carriers of one sign to become Mn^{3+} or Mn^{+} ; then the oppositely charged carrier would be captured to form Mn^{++} in an excited state.

The free charge density n , produced by either of these mechanisms can be computed from the relation,

$$n = \frac{1}{Suz} \frac{dz}{dt} \quad (6)$$

Here z is the number of color centers or Mn^{++} ions at which recombinations can occur. S is the capture cross section for recombination, and u is the thermal velocity of the charge carriers (10^7 cm/sec at 350°K).

For case (1), z and dz/dt can be determined from bleaching curves like those in Fig. 5. For case (2), z can be determined from Mn^{++} content, corrected for concentration quenching¹; and dz/dt can be determined from glow curve data.

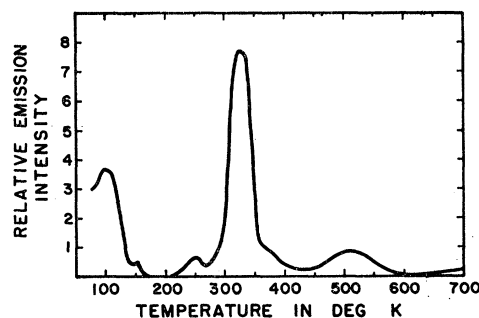


Fig. 10. Glow curve of a high purity, synthetic calcite sample.

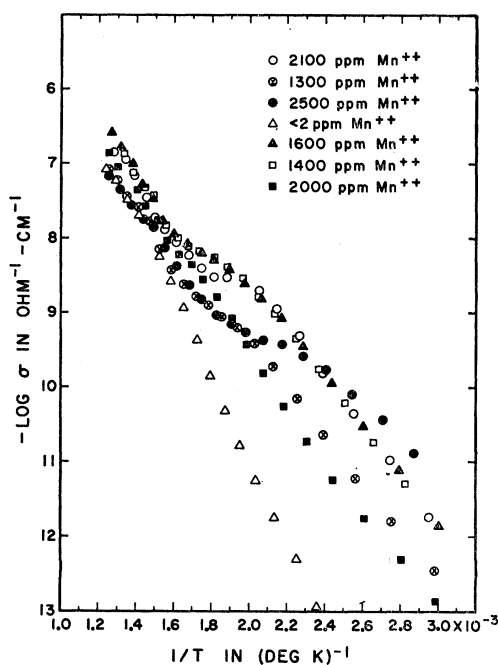


FIG. 11. Conductivity curves of several crystals irradiated at room temperature for 2 h.

The crystals containing 1300 and 2000 ppm Mn^{++} in Fig. 11 gave the most conclusive results from such calculations since their ionic conductivity was lowest. Absorption and glow curve data for these crystals were roughly identical. After two hours of room-temperature irradiation the bleaching rate at $350^\circ K$ gave $dz/dt = 5 \times 10^{14} \text{ sec}^{-1}$ for case (1). The subsequent decrease in absorbance corresponded to $z = 7 \times 10^{16} \text{ cm}^{-3}$. If we assume S to be no larger than 10^{-15} cm^2 for the color centers,¹¹ this gives $n \geq 10^6 \text{ cm}^{-3}$.

Comparing the $350^\circ K$ glow peak intensity with a source of known brightness gave $dz/dt = 3 \times 10^{14} \text{ sec}^{-1}$ for case (2). Mn^{++} content, corrected for concentration quenching, gave $z = 10^{17} \text{ cm}^{-3}$ for both crystals. Again, taking $S \leq 10^{-15} \text{ cm}^2$ for Mn^{++} centers,¹² we find $n \geq 3 \times 10^5$.

Assuming a free charge mobility v of $10 \text{ cm}^2/\text{V sec}$ for calcite, these results correspond to conductivities of no less than $8 \times 10^{-12} \Omega^{-1} \text{ cm}^{-1}$ for case (1) and $3 \times 10^{-12} \Omega^{-1} \text{ cm}^{-1}$ for case (2). Conductivity peaks of this magnitude would be readily detectable in the curves of Fig. 11. But since the values of S could be larger than assumed, the conductivity data are by no means conclusive.

On the other hand, glow curve measurements show that there is no change in thermoluminescence intensity in any of the glow peaks during application of voltage pulses to single crystals. This was verified for fields of

up to $10\,000 \text{ V/cm}$. Fields of this magnitude are expected to alter the capture cross sections of both recombination centers and Mn^{++} ions.¹³ This would affect the recombination rates, and hence the thermoluminescence intensity, for either of the above mechanisms. The absence of any such effect is good evidence that free charge carriers are not involved in the bleaching or emission processes.

The conductivity data in Fig. 11 are characteristic of ionic crystals whose conduction is due to mobility of vacancies. The curves show the usual structure-sensitive and intrinsic regions. The data in each region are consistent with much older results published by Joffe¹⁴ and by von Rautenfeld.¹⁵

V. DISCUSSION

Since none of the calcite color centers are optically bleached or produce photoconductivity, absorption must involve only transitions to bound excited levels. The strong dichroism of the $2950\text{-}\text{\AA}$ band means that its absorption is almost certainly associated with carbonate ions. Impurities, vacancies, or other defects cannot be expected to account for such a large degree of anisotropy. It is reasonable to assume then, that this band is due to CO_3^- ions formed near lattice inhomogeneities as proposed by Kolbe and Smakula.⁸ Presumably, the $2950\text{-}\text{\AA}$ band is due to transitions between the ground state and the first excited state of this trapped-hole center.

The $3500\text{-}\text{\AA}$ band can be attributed to transitions between the ground state and lowest excited level of isotropic centers. Undoubtedly, these are trapped-electron centers⁸ since they are annihilated simultaneously with the trapped-hole centers. The remaining uv bands are bleached simultaneously with the 2950- and $3500\text{-}\text{\AA}$ bands and show little or no dichroism. Therefore, they are probably due to transitions between the ground state and higher excited levels of the trapped-electron centers.

We assume that thermal bleaching occurs when oppositely charged centers acquire enough mobility to move within recombination range of one another. Evidently, recombination occurs through a localized process such as tunneling, which does not involve charge transfer. If the color centers are assumed to be Ca^+ and CO_3^- ions, the Ca^+ ions are expected to be the mobile centers. High-temperature measurements of transference numbers in calcite show that Ca^{++} ions carry the ionic current above $600^\circ C$.¹⁶ Also, according to high-temperature measurements,¹⁷ the diffusion co-

¹³ H. F. Ivey, *Electroluminescence and Related Effects* (Academic Press Inc., New York, 1963), p. 181.

¹⁴ A. Joffe, *Ann. Physik* **72**, 461 (1923).

¹⁵ F. von Rautenfeld, *Ann. Physik* **72**, 617 (1923); *Z. Tech. Physik* **5**, 524 (1924).

¹⁶ A. Joffe, *The Physics of Crystals* (McGraw-Hill Book Company, Inc., New York, 1928), p. 124.

¹⁷ R. A. W. Haul and L. H. Stein, *Trans. Faraday Soc.* **51**, 1280 (1955).

¹¹ N. F. Mott and R. W. Gurney, *Electronic Processes in Ionic Crystals* (Oxford University Press, London, 1948), 2nd ed., p. 108.

¹² A. Rose, *Phys. Rev.* **97**, 322 (1955). R. H. Bube *Photoconductivity in Solids* (John Wiley & Sons, Inc., New York, 1960), p. 61.

efficient for CO_3^- ions in calcite is $D=4.5\times 10^{-4} \exp(-58\,000/RT)$ over the range 600–850°C. From the Nernst-Einstein equation, the corresponding electrical conductivity would be $\sigma=2.1 \exp(-3.8\times 10^{-12}/kT)$. This gives values much too small to account for the conductivities at 550°C in Fig. 11. Therefore, CO_3^- ions evidently make negligible contribution to the ionic conductivity at this temperature; and it is reasonable to assume the same at lower temperatures. It follows that CO_3^- mobility should also be much smaller than Ca^+ mobility at 350°K.

Figures 4 and 5 show that there are at least four stages of thermal bleaching and that the 3500-Å band is shifted during each one. This is interpreted to mean that there are four kinds of electron-trapping centers. Each of the bleaching stages is then attributed to annihilation of one kind of electron-trapping center through recombinations which use up a portion of the trapped-hole centers. The problem remains, however, of explaining how there can be four or more kinds of Ca^+ centers which can give rise to such a large spread of bleaching temperatures. One possibility is to assume that Ca^+ ions are formed in regions having different degrees of lattice deformation. Under these conditions, it is conceivable that mobility would set in at well separated temperatures for each kind of site.

Excitation of Mn^{++} ions during annihilation of the color centers apparently does not involve charge transfer. Therefore, possible mechanisms seem to be limited to (1) a completely localized charge transfer process, or (2) energy transfer.

Localized charge transfer can only occur if the Mn^{++} ions and color centers are part of the same complex. This is contradicted by lack of correlation between Mn^{++} content and absorbance data. It is also inconsistent with the large variations in thermoluminescent efficiency of Table I. These variations could only be accounted for by assuming that variable fractions of color center complexes contain Mn^{++} ions. Crystals with inconsistently high absorbance would be those with largest fractions of such centers. Therefore, these crystals should have the smallest $\Delta x/\Delta z$ ratios in Table I; however, no such correlation was found.

Therefore, energy transfer between recombination sites and Mn^{++} centers is the most plausible excitation mechanism. Evidently, the same nonradiative resonance transfer process which produces sensitized luminescence in Mn-activated calcite⁴ is involved. The

efficiency of this process is proportional to r^{-6} , where r is distance between recombination site and Mn^{++} ion.¹⁸ Thus, the high transfer efficiencies indicated by Table I can only be explained by nonrandom distributions of Mn^{++} ions and recombination centers. This is not unlikely and would also account for the large variations in excitation efficiency of Table I.

Results of the decay of absorbance and phosphorescence at room temperature are at variance, in some respects, with a simple bimolecular recombination of trapped holes and electrons. Earlier work¹⁹ based on a monomolecular trap-emptying process involving distributions of trapping energies is also inconsistent with present results. However, both models explain many observed results. Therefore, the next logical step is to consider a model based on bimolecular recombination with a distribution of activation energies.

VI. CONCLUSIONS

Thermoluminescence in calcite is closely associated with the presence of x-ray induced, uv absorption bands. These bands are stable at liquid-nitrogen temperature but are simultaneously bleached by heating to 750°K. This thermal bleaching occurs in four stages which coincide with each of the prominent glow peaks. Polarized absorption spectra indicate that the absorption bands are due to four kinds of trapped-electron centers and one kind of trapped-hole center. Each stage of thermal bleaching can be attributed to recombinations involving a portion of the trapped-electron centers and one kind of trapped-hole center. Thermoluminescence is produced when the recombination energy excites Mn^{++} impurity ions. The recombination and excitation processes do not involve charge transfer. Also, the efficiency of excitation due to recombination is generally high and quite variable between different glow peaks and in different samples. These and other results are consistent with an excitation mechanism involving nonradiative resonance transfer of energy between recombination sites and emission centers.

ACKNOWLEDGMENTS

The author wishes to thank J. M. Waite, W. H. Shelton, and R. D. Roland for their help and Socony Mobil Oil Company for permission to publish this paper.

¹⁸ D. L. Dexter, J. Chem. Phys. **21**, 836 (1953).

¹⁹ W. L. Medlin, Phys. Rev. **123**, 502 (1961).